

THE GEOMETRY OF BACK ARC THRUSTING ALONG THE EASTERN SUNDA ARC, INDONESIA:  
CONSTRAINTS FROM EARTHQUAKE AND GRAVITY DATA

Robert McCaffrey and John Nábělek

Department of Earth, Atmospheric and Planetary Sciences,  
Massachusetts Institute of Technology

**Abstract.** The Flores earthquake of December 23, 1978, represents the first seismological evidence for active back arc thrusting behind the eastern Sunda Arc. This  $m_b = 5.8$  earthquake occurred north of Flores Island, where seismic reflection profiling has revealed back arc thrusting, interpreted to be a reaction to compression of the arc following collision with the Australian continent. We investigate the source mechanism and depth of the Flores earthquake by inversion of long-period P waveforms and relocate the earthquake's epicenter incorporating arrival time data from local stations. We find that this event occurred beneath the accretionary prism south of the back arc thrust zone at a depth of 11.5 km (7 km below the seafloor). The best fitting fault plane solution is consistent with active southward thrusting of the floor of the Flores Basin beneath the volcanic arc along a 30° dipping fault plane. The morphology of the thrust zone and the free-air gravity profile over the Flores Basin in the epicentral region resemble those of oceanic trenches, and the observed gravity field is best interpreted if the crust of the Flores Basin dips smoothly below the accreted wedge at an average angle of about 6°. The position of the earthquake hypocenter south of the Flores Thrust and the fault plane solution suggest that the 1978 earthquake is analogous to thrust events at subduction zones and represents slip between the subducting and overriding plates. The Flores Thrust is thus the surface expression of a deep-seated thrust zone and may represent the initial stage of polarity reversal of the eastern Sunda Arc.

Introduction

One of the consequences of plate motions is the eventual involvement of continents and their fragments in convergence zones. A few areas of the world are thought to derive their structural complexity from the attempted subduction of continental crust, but the details of the process are far from obvious. Involvement of these nonsubductable terrains in a convergent boundary may not always result in a large-scale deformation as in the continent-continent collision between India and Asia, but is nevertheless likely to trigger changes in the subduction regime.

McKenzie [1969] suggested that attempted subduction of continental lithosphere beneath an oceanic island arc might result in reversal of subduction polarity because the buoyancy of the continental crust would prevent it from being

subducted. A likely place for this to have happened in the past is northern New Guinea during the Tertiary [Dewey and Bird, 1970; Johnson and Molnar, 1972; Hamilton, 1979], but reversal is not required [Johnson and Molnar, 1972; Johnson and Jaques, 1980]. Reversal may also be underway behind the Sangihe Arc in the northern Molucca Sea [Silver and Moore, 1978; Stewart and Cohn, 1979; Moore and Silver, 1983] following a collision between island arcs. Arc polarity reversal is undoubtedly difficult to identify and prove from the geologic record alone, and thus it is important to study any modern example of where it may possibly be occurring.

Probably the best area to study the incipient subduction of continental material and back arc thrusting is the eastern Sunda Arc, where Australia is presently impinging on the subduction zone. South of Timor and around the great bend in the Banda Arc to the north, continental crust of Australia is found seaward of the Timor Trough (Figure 1) and extends arcward to beneath the trough itself [Jacobson et al., 1979]. Reflection profiles crossing the Australian shelf and the Timor Trough show typical subduction zone morphology and clearly indicate thrusting of Australia beneath the deformed outer arc ridge (which includes Timor) south of the volcanic islands [Jacobson et al., 1979; von der Borch, 1979; Hamilton, 1979; Bowin et al., 1980]. West of Sumba, oceanic lithosphere of the Indian Ocean plate is being consumed at the Java Trench. The presence of the Scott Plateau, possibly a subsided block of the Australian shelf, and Sumba, possibly a continental fragment caught in the fore arc, adds a great deal of complexity to the convergent margin in the transition zone between the Java Trench and the Timor Trough.

Because of the young age of Australia's collision with the eastern Sunda Arc, it has thus far caused only small morphological changes in the subduction system. The available evidence indicates that back arc thrusting has been initiated [Hamilton, 1979; Usna et al., 1979; Silver et al., 1983] that may eventually result in either reversal of the subduction polarity, thus removing the back arc basin from the surface of the earth, or in crustal thickening by imbricate thrusting, thereby producing a belt of ophiolites. The present mode of deformation appears to favor the former scenario.

North of the Sunda island arc from western Sumbawa to east of Wetar (except for a small stretch between east Flores and Alor), seismic reflection profiling has revealed thrusting at the base of the slope of the volcanic pile (Figure 1) [Silver et al., 1983]. The sense of thrusting is such that oceanic crust of the Flores Basin and the Banda Sea is being over-

Copyright 1984 by the American Geophysical Union.

Paper number 4B0541.  
0148-0227/84/004B-0541\$05.00

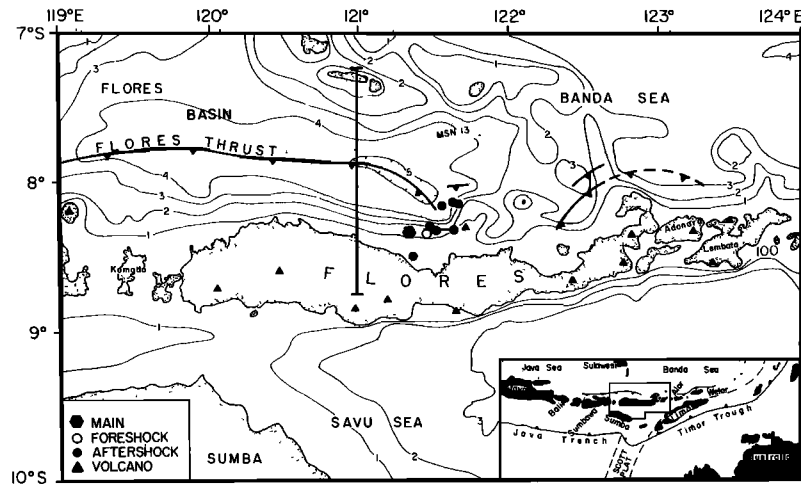


Fig. 1. Location map (insert) and detailed map of the Flores region. Thrust faults are indicated by solid lines with barbs on the overriding plate, and bathymetric contours are in kilometers [from Silver et al., 1983]. The dashed line in the inset shows the inferred northwestern limit of Australian continental crust (and the Scott Plateau) beneath the outer arc ridge [from Hamilton, 1979]. The large hexagonal symbol shows the calculated epicenter of the 1978 earthquake. The north trending heavy line is the position of the profile of Figures 5 and 6. The dotted line north of the Flores thrust is the location of seismic refraction profile MSN-13.

ridden by the volcanic islands. Silver et al. [1983] estimate the amount of convergence between the Flores Basin and the island arc in the Flores region at 30-60 km based on the volume of material accreted to the toe of the volcanic arc. This length is consistent with the amount of northward indentation of this portion of the arc with respect to those portions behind which thrusting is not observed. There is, however, no evidence that this thrust zone is associated with a southward dipping zone of intermediate-depth earthquakes [Cardwell and Isacks, 1978].

In this paper we discuss an  $m_b = 5.8$  earthquake from the thrust zone north of Flores; its fault plane solution constitutes the first seismological evidence to support interpretations that active back arc thrusting occurs behind the Sunda Arc. Also, simple models for the structure of the back arc thrust zone that satisfy gravity data and published seismic refraction and reflection profiles are presented. These data suggest that the crust (probably oceanic) of the Flores Basin either dips beneath the small back arc accretionary prism at an angle of about  $6^\circ$  or thickens considerably under the southern Flores Basin. The presence of a large negative  $-1.10 \text{ mm/s}^2$  ( $-110 \text{ mGal}$ ) free-air anomaly over the accreted wedge 30 km south of the bathymetrically deepest part of the Flores Basin signifies that the crust is out of isostatic equilibrium and suggests the underthrusting plate is flexed down as in more developed subduction zones. The position of the earthquake hypocenter south of the Flores Thrust and the fault plane solution indicate that the 1978 earthquake was due to southward underthrusting of the Flores Basin crust beneath the overriding island arc.

#### The Earthquake of December 23, 1978

##### Location

The earthquake of December 23, 1978, together with one foreshock and seven aftershocks, was

relocated using arrival time data from the regional network of Indonesia and southeast Asia [Hodgson, 1980], from a local network operating on Sulawesi [McCaffrey and Sutardjo, 1982], and from International Seismological Centre (ISC) bulletins. We repicked arrival times for all regional and many of the World-Wide Standardized Seismograph Network (WWSSN) stations. The main shock was located at latitude  $8.33^\circ\text{S}$ , longitude  $121.34^\circ\text{E}$  (Figure 1) and origin time 0510:50. This epicenter is only 8 km southwest of the ISC reported epicenter. The earthquake's depth was fixed at 11 km in these calculations as determined from the body wave analysis discussed below. The depth reported by the ISC was 7 km based on P wave arrival times and 31 km from pP-P times.

Our calculated location of the event of December 23 is about 30 km south of the eastern end of the Flores Thrust (Figure 1). Since the regional structure is oriented east-west, the uncertainty in the location due to lateral variations in the velocity structure is probably greater in the north-south direction. Clear P arrivals at stations in central Sumba, western Timor, and southern Sulawesi, however, give strong control on the epicenter. The absence of reported damage on Flores and the presence of strong water reverberations in the P wave seismograms (discussed below) indicate that the earthquake occurred beneath the sea and not beneath Flores Island. Furthermore, the period of the water reverberations requires a water depth of about 4.5 km, which implies that the epicenter was at least 15 km to the north or northwest of that determined from the arrival time data (Figure 1).

The foreshock and aftershocks were relocated relative to the main shock by the method of joint hypocenter determination [Dewey, 1971]. The depths of these events were fixed at 15 km for lack of independent depth information, but the choice of any depth above 50 km for these events

TABLE 1. Source Parameters Determined From the Inversion of P Waves Using Different Source Parameterizations and Choices for the Error Function\*

Moment Tensor						
Error Function 1						
Normalized moment-tensor components:				Principal axes:		
				Eigenvalue	Azimuth	Plunge
$M_{xx} = -0.51 \pm 0.03^\dagger$	$M_{xy} = -0.11 \pm 0.07$	P	$-0.65 \pm 0.04$	$9 \pm 7^\circ$	$17 \pm 1^\circ$	
$M_{yy} = -0.10 \pm 0.03$	$M_{xz} = -0.40 \pm 0.02$	T	$0.75 \pm 0.02$	$156 \pm 5^\circ$	$70 \pm 1^\circ$	
$M_{zz} = 0.61 \pm 0.01$	$M_{yz} = 0.09 \pm 0.02$	B	$-0.10 \pm 0.04$	$276 \pm 6^\circ$	$10 \pm 4^\circ$	
Moment-tensor norm = $2.61 \pm 0.30 \times 10^{18}$ N m    Depth = $11.5 \pm 0.3$ km						
Decomposition: <sup>‡</sup> Double couple = 87%    Linear vector dipole = 13%						
Amplitudes of the source time function elements: <sup>§</sup>						
0.23 $\pm$ 0.01, 0.37 $\pm$ 0.03, 0.29 $\pm$ 0.02, 0.13 $\pm$ 0.01, -0.02 $\pm$ 0.02						
Constrained Double Couple						
Error Function	Depth (km)	Scalar moment ( $10^{18}$ N m)	Strike (deg)	Dip (deg)	Rake (deg)	Amplitudes of source time function elements
1	11.4 $\pm$ 0.4	1.83 $\pm$ 0.08	114 $\pm$ 9	30 $\pm$ 2	114 $\pm$ 6	0.24 0.40 0.26 0.14 -0.04 ( $\pm$ 0.02)
2	10.1 $\pm$ 0.3	1.69 $\pm$ 0.10	117 $\pm$ 6	32 $\pm$ 1	115 $\pm$ 3	0.34 0.48 0.19 0.06 -0.07 ( $\pm$ 0.02)

\* The two choices for the error function are discussed in the text.

† All quoted uncertainties represent one standard deviation.

‡ The moment tensor is constrained to be purely deviatoric.

§ The duration of each source time function element is 2.0 s.

has little effect on the epicentral location. The foreshock and aftershocks appear to have been concentrated to the northeast of the main shock, closer to the eastern termination of the Flores Thrust (Figure 1) as mapped by reflection profiling [Silver et al., 1983]. The apparent northeast trend of the epicenters may be fictitious since the 95% confidence ellipses for most of the relocations are aligned in that direction.

#### P wave Analysis

Long-period P waves from the vertical component of 10 WWSSN stations were inverted simultaneously for the orientation of the double-couple source, the centroid depth and the far-field source time function. The source time function was parameterized by a series of box-car elements, each 2.0 s in duration (this parameterization is identical to that by Langston [1981]). Data were inverted with two choices for the error function that was minimized in a least squares sense: (1)  $o_i - s_i$  and (2)  $o_i/(\sum o_j^2)^{1/2} - s_i/(\sum s_j^2)^{1/2}$ , where  $o_i$  are the amplitudes of the digitized observed waveforms and  $s_i$  are the corresponding synthetic seismogram amplitudes. The summations with respect to  $j$  are made over the number of data points at a given station. The first error function uses information contained in the amplitude variation between the stations, while the second is sensitive only to the shapes of the seismograms. When the second error function is used, the seismic moment is determined by matching the original unscaled data in the least squares sense with the synthetic seismograms determined during the final iteration. Details of these procedures are de-

scribed by Nábělek [1984] and are similar to those used by Langston [1981] and Ward [1980], the main difference being that the source depth is also determined in our inversion procedure.

Observed seismograms were digitized at half-second intervals and filtered with a highpass filter with cutoff at 0.017 Hz in order to remove the low-frequency drift that was observed at some stations. The first 60 points (30 s) from the onset of the direct P wave were used for the analysis. The onset of the P arrival was determined from the short-period seismograms but was allowed to vary by up to 1.5 s if improved cross correlation between the observed and synthetic waveforms could be found. Because the inversion using a full moment tensor source yielded an almost pure double couple mechanism, the double couple constraint was subsequently applied. The solutions using either the moment tensor or constrained double couple source, and either choice of the error function are essentially identical (Table 1). The estimated parameters for the source centroid are depth 10-12 km, strike 105-120°, dip 28-32°, and rake 105-120°. The largest contribution to the total seismic moment comes from the first four elements of the source time function; the rupture duration was therefore about 8 s. The seismic moment is  $1.5-2.2 \times 10^{18}$  N m, the exact value being sensitive to the estimate of the source depth. Estimates of the uncertainties above are based on formal variances for a given model and on variations in solutions using different error functions and different acceptable crustal models; they are therefore larger than the formal uncertainties given in Table 1. The north dipping nodal plane is clearly the better resolved

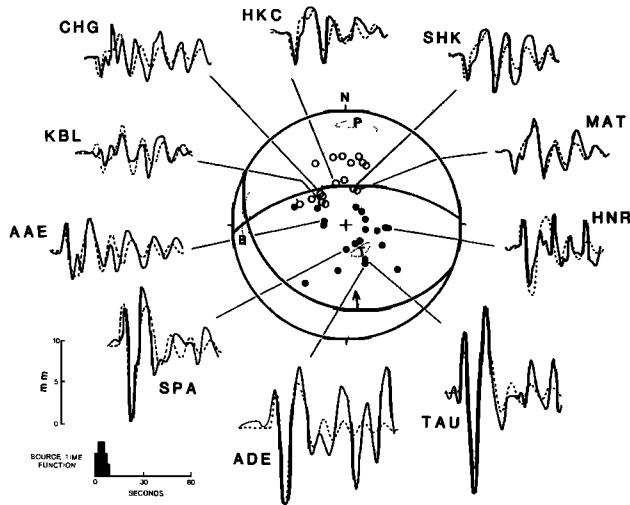


Fig. 2. Observed (solid lines) and synthetic (dashed lines) long-period P waves and the best fit fault plane solution for the 1978 Flores earthquake. The bars on the time scale represent the source function in 2.0-s intervals. The amplitude scale for the seismograms is in millimeters at a magnification of 3000 and epicentral distance of  $40^\circ$ . Also shown is a lower hemisphere plot of first motion polarities. Solid circles represent compressional first motions, and open circles are dilatations. The dotted lines enclose the possible orientations of the P, T, and B axes as labeled. The arrow shows the horizontal projection of the slip vector.

of the two. An attempt was made to identify the actual fault plane from the waveform distortion that would be expected from rupture propagating along a finite fault plane, but the results were inconclusive. Other evidence, discussed below, suggests that the south dipping nodal plane is the fault plane.

Observed and synthetic seismograms for the best fitting fault plane solution are shown in Figure 2. The observed and theoretical seismograms have been corrected to equal distance ( $40^\circ$ ) and instrument magnification ( $\times 3000$ ). Also shown are first motion polarities for P waves that were read for many more stations, and the uncertainties in the P, T, and B axes. The synthetic seismograms were generated using the source crustal structure shown in Table 2. This structure is based on the seismic refraction profile MSN-13 (Figure 1) of Curray et al. [1977]. A value of 1 s was used for  $t^*$  (the ratio of travel time to average Q) to account for anelastic attenuation in the earth.

Although the synthetic seismograms at the northern stations appear to satisfy the dilatational first motions observed on the short-period instruments (a dilatational direct P is clearly visible on the short-period record from MAT), the synthetic direct P arrivals at these stations are in fact compressional. The first discernible pulse in the long-period records at these stations corresponds to a strong dilatational pP (P wave reflection from the sea floor), which because of the shallow focus of this event, obscures the direct P arrival [Tréhu et al.,

1981]. The discrepancy between the short-period first motion data and those predicted by our model is probably real. Short-period first motions are indicative of the source orientation at the nucleation point of the rupture, which may differ from the average orientation of the fault plane. The long-period data, however, are indicative of the average orientation. Some variability in the source orientation is to be expected considering the long duration of rupture (8 s), hence a fault length of at least 20 km.

A change in the direction of slip could also be responsible for the small oscillation observed in the first few seconds of the long-period waveform at KBL (Figure 2) that cannot be accounted for with our point source model. Alternatively, the precursor at KBL may be explained by multipath ray propagation through the high-velocity slab of the subducting Indian Ocean plate that dips to the north beneath the epicentral region because the paths of the rays arriving at this station parallel the strike of the slab.

In order to investigate the sensitivity of the waveforms to the source depth, we performed the inversion at fixed 5-km increments above and below the best fitting depth (Figure 3). In terms of the rms residual, the source depth at 11.5 km represents about a 10% improvement over the solutions at assumed source depths both 5 km shallower and deeper.

The complexity of the latter part of the waveforms is mainly due to reverberations within the water column. The period of these reverberations provides strong constraint on the depth of the water above the hypocenter, which in turn, provides a constraint on the epicentral location when used with bathymetric charts. Figure 4 shows seismograms generated for three water depths compared to those observed at stations AAE and MAT. The best fit to the period of the observed reverberations is at a water depth of 4.5 km; thus this depth was used in calculating all seismograms and implies a more northerly location for the epicenter than that determined from travel time data (Figure 1).

#### Structure in the Epicentral Region

The Flores earthquake of December 23, 1978, occurred in the region north of Flores, where there are large negative free-air gravity anomalies over a small but distinct trench and its associated deformed accretionary prism. The

TABLE 2. Crustal Structure Used in the Calculation of the Synthetic Seismograms

	Thickness (km)	$v_p$ (km/s)	$v_s$ (km/s)	Density ( $\times 10^3$ kg/m <sup>3</sup> )
Source region				
	4.5	1.51	0.00	1.03
	2.0	3.20	1.31	2.30
	half-space	6.10	3.10	2.90
Receiver region				
	half-space	6.00	3.46	2.80

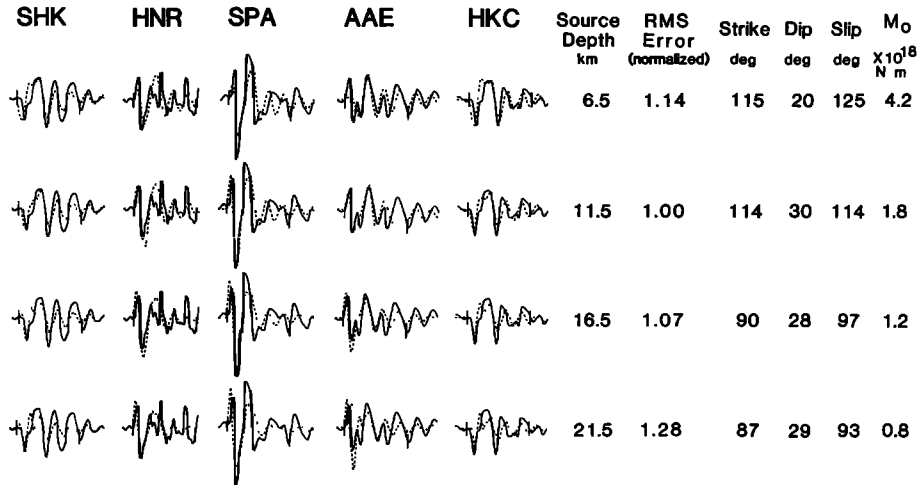


Fig. 3. Results of inverting for source parameters with source depth fixed at 5-km intervals. Solid lines are observed, and dotted lines are calculated seismograms. The depth of 11.5 km was determined by the inversion with the source depth as one of the free parameters and provides the best fitting depth. The rms errors listed are scaled to the minimum value (that for 11.5 km).

strong correlation between the presence of the back arc trench and free-air gravity lows behind the Sunda Arc suggests that the lows result from depression of the crust of the Flores Basin in the process of underthrusting below the arc [Silver et al., 1983]. The gravity lows are most strongly developed north of western Flores over the epicentral region of the earthquake described in this paper. Here, free-air gravity anomalies reach below  $-1.10 \text{ mm/s}^2$  ( $-110 \text{ mGal}$ ) with the minimum centered over the accretionary prism south of the trench rather than over the bathymetric low of the back arc trench (Figure 5a). In this section we explore crustal structure in the vicinity of the December 23 earthquake by generating simple models satisfying seismic refraction (profile MSN-13 of Curray et al. [1977]), seismic reflection, bathymetric, and free-air gravity data north of Flores [Silver et al., 1983], and Bouguer gravity data on Flores [Geological Research and Development Centre, 1984].

In computing the gravity effect of our two-dimensional models, densities were estimated from seismic velocities obtained from refraction profile MSN-13 and the compressional velocity-density relations of Nafe and Drake [1963] for the sediment layer and of Christensen and Salisbury [1975] for oceanic crustal rocks. We assume that the lowest interface from profile MSN-13 ( $7.7 \text{ km/s}$  at  $14\text{-km}$  depth) represents the Moho, but because the density for oceanic crustal rocks of that seismic velocity is close to that of upper mantle rocks [Christensen and Salisbury, 1975], the distinction between rock types is not critical for the purposes of the density model.

The starting model was an isostatically balanced section across the Flores Basin (Figure 5b). The crustal and sediment thicknesses beneath the central Flores Basin were taken from refraction profile MSN-13 that crosses the gravity profile at about  $\text{km } 70$  (Figures 1 and 5b). The crust was assumed to be oceanic (i.e.,  $7 \text{ km}$  thick based on MSN-13) where water depths exceed  $4 \text{ km}$  and to thicken toward the north and south reaching  $34 \text{ km}$  beneath the coastlines at both edges of the profile. Seafloor topography shows up strongly as short-wavelength gravity anomalies, suggesting a lack of local compensation. The match in amplitudes between observed and calculated anomalies over bathymetric features validates our choice of sediment density. We also included the effect of the subducted Indian Ocean plate, which is likely to have a long-wavelength positive contribution to the gravity field across the profile. The assumed slab geometry (Figure 5c) is based on seismic zone contours from Cardwell and Isacks [1978], a density contrast of  $0.05 \times 10^3 \text{ kg/m}^3$  between the slab and asthenosphere [Grow and Bowin, 1975], and a thickness of  $50 \text{ km}$ . The computed gravity effect of the subducted Indian Ocean plate is  $0.54 \text{ mm/s}^2$  ( $54 \text{ mGal}$ ) over Flores Island and decreases to  $0.38 \text{ mm/s}^2$  over the northern end of the profile, constituting a gradient of only  $0.001 \text{ mm/s}^2$  per  $\text{km}$  ( $0.1 \text{ mGal/km}$ ). The addition of

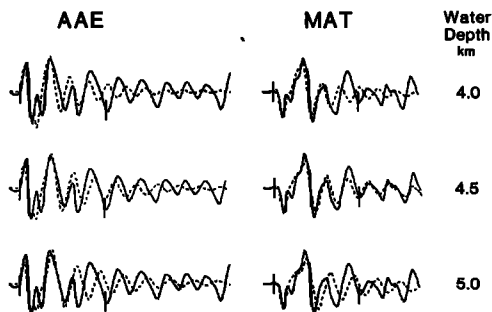


Fig. 4. Observed (solid lines) and synthetic (dotted lines) P wave seismograms generated for water depths of  $4.0$ ,  $4.5$ , and  $5.0 \text{ km}$ . Crustal structure is otherwise as shown in Table 2, and the source parameters are the same as the  $11.5 \text{ km}$  depth source in Figure 3. A good agreement in period of the water reverberations occurs for a water depths of  $4.5 \text{ km}$ .

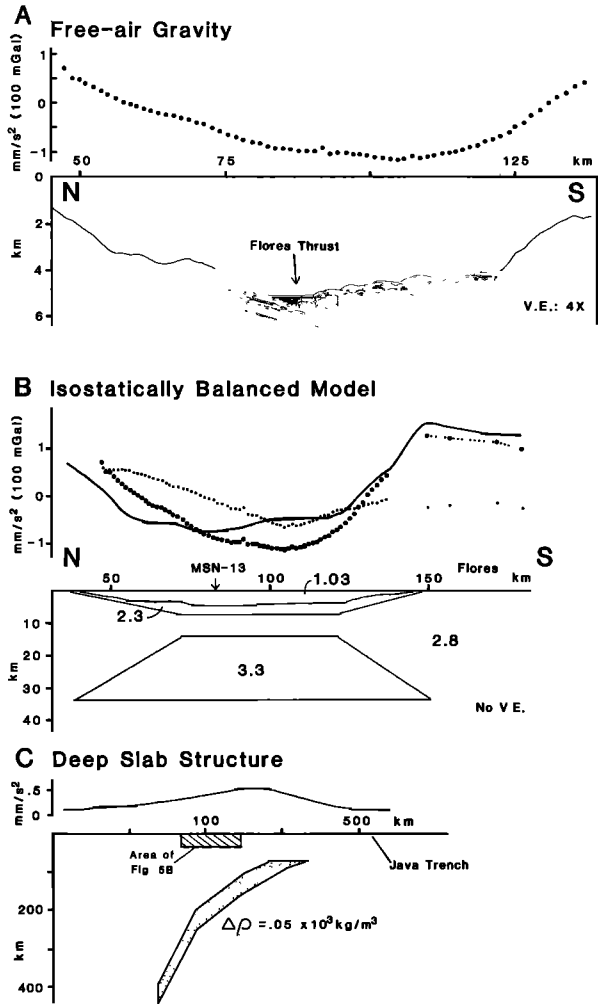


Fig. 5. (a) Free-air gravity profile and line drawing interpretation of seismic reflection profile across the Flores thrust zone [from Silver et al., 1983]. The position of this profile is shown in Figure 1. (b) Comparison of computed gravity profile for an isostatically balanced crustal model (solid curve) with the observed profile (large dots). Note the strong linear trend in the residuals (small dots). Assumed densities (in units of  $10^3 \text{ kg/m}^3$ ) are given for each layer. The isostatically balanced crustal model assumes an average density of  $2.8 \times 10^3 \text{ kg/m}^3$  to a depth of 34 km. Gravity anomalies are free-air over the Flores Basin and Bouguer over Flores Island. (c) Deep slab structure assumed in all calculations and its gravity effect. All horizontal axes are labeled with a common origin.

the positive gravity effect of the slab improves the fit to the observed gravity anomalies over the islands at the ends of the profile which are too positive to be accounted for by the isostatically balanced crustal model alone.

Relative to the isostatically balanced model with the effect of the subducted Indian Ocean plate included, there is a southward decreasing gradient of  $0.020 \text{ mm/s}^2$  per km ( $2.0 \text{ mGal/km}$ ) over the northern Flores Basin and a total drop in the gravity field of approximately  $0.70 \text{ mm/s}^2$  ( $70$

$\text{mGal}$ ) over the southern Flores Basin (Figure 5b). The residual low relative to the isostatically balanced model is centered over the accretionary wedge and not over the bathymetric low of the trench, suggesting that the crust of the Flores Basin continues to thicken or dip southward below the deformed sediments. The gravity low over the southern Flores Basin requires a mass deficiency beneath the Flores Thrust zone. The requisite crustal thickening can occur either by scraping sediments off the plate as it thrusts coherently beneath the sediment pile along a single, shallow dipping decollement or by a series of imbricate thrust faults involving both the basement and sediment rocks.

The decollement model (Figure 6a) is generated by assuming that the oceanic crust of the Flores Basin is of constant thickness as it thrusts beneath the accretionary wedge. In this case the increase in crustal thickness occurs by down-bowing of the oceanic crust beneath the thrust zone as sediments are accreted to the overlying deformed wedge. In Figure 6a, the crust of the Flores Basin beneath the site of refraction profile MSN-13 agrees in general with those results, and from this point dips to the south at about  $6^\circ$ , reaching a maximum depth of 10.0 km beneath the minimum in the gravity field. The dip angle of  $6^\circ$ , which is likewise the dip angle of the planar sediments south of the Flores Thrust (see the seismic reflection profile in Figure 5a), provides the best fit (within  $1^\circ$ ) to the gravity data. The gravity data thus suggest that underthrusting at this dip angle continues tens of kilometers south of the deformation front.

It is interesting that the dip angle determined here is similar to that of many subducting plates at trenches in the western Pacific [Watts and Talwani, 1974]. By analogy we suggest that the Flores Basin lithosphere behaves as an elastic plate while thrusting beneath the island arc and that the large gravity anomalies are due to bending of the plate in response to vertical forces applied to the underthrust portion of the plate. Because the free-air gravity anomalies are negative almost as far south as the north coast of Flores, the load of the crustal material between Flores Island and the Flores Thrust cannot by itself account for the deflection of the Flores Basin lithosphere. Therefore either the underthrusting plate extends as far south as Flores Island or the plate's own gravitational instability aids to pull it into the asthenosphere.

A second mechanism one could envision is the case of a thickened crust perhaps resulting from imbricate thrusting where shortening is taken up along a series of south dipping thrust faults that penetrate both the basement and the sedimentary section. In this case the thickened crust would be comprised of both oceanic crust and sediments. The crustal model in Figure 6b was generated by assuming that the increased thickness of crust beneath the Flores Thrust zone consists of 30% sediment and 70% oceanic crust, in the same proportions as the undisturbed crust that enters the thrust zone. Clearly, this type of model can satisfy the gravity data equally as well as the decollement model. Contrary to the decollement model, closure of the Flores Basin in

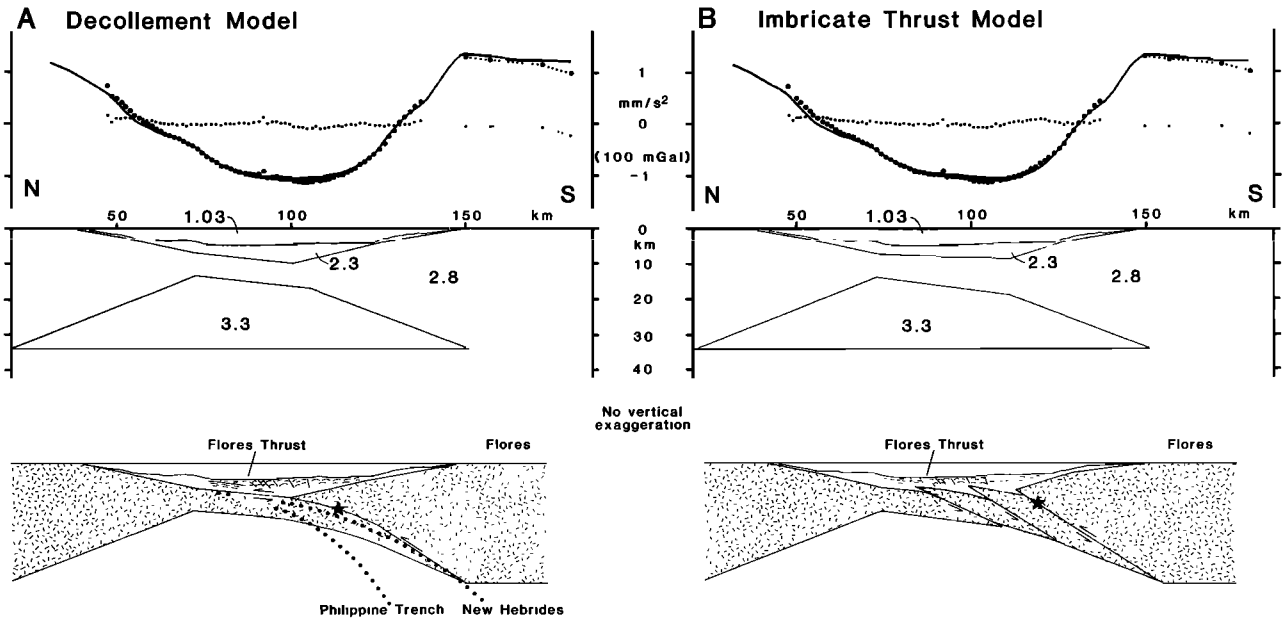


Fig. 6. Alternative models for the structure of the back arc thrust zone. (a) The decollement model where crustal thickening occurs by deflection of the overriding plate and sediment accretion, and (b) the imbricate thrust case in which both oceanic crust and sediments comprise the thickened crust. Presentation of density models is the same as in Figure 5b. At the bottom are cartoon interpretations of the density models. A star shows the inferred position of the 1978 earthquake shifted from its calculated position relative to the crustal models to a position beneath 4.5 km of water as required by the period of reverberations in the waveforms. Dotted lines in the bottom panel of Figure 6a show the projections of the New Hebrides and Philippine Trench seismic zones at the same scale for purposes of comparison. For reasons discussed in the text, the decollement model is preferred.

this fashion would leave its mark in the geologic record as an ophiolite belt sandwiched between two volcanic belts (i.e., Flores and Sulawesi). The increase in the cross-sectional area of the crust shown in Figures 5a and 5b accounts for about 30 km of crustal shortening if the crust entering the thrust zone is 10 km thick initially.

An unlikely alternative is based on the assumption that the north dipping P wave nodal plane of the 1978 earthquake is the fault plane. This implies that Flores Island thrusts beneath the Flores Basin along steeply dipping reverse faults. We consider this scenario highly unlikely because buoyancy forces at the contact between the different crustal types would tend to push the less dense island arc crust out over the oceanic crust when external horizontal compressive forces are applied. Also, the seismic reflection profile in Figure 5a clearly shows planar sediments from the north side dipping southward below the accreted wedge.

#### Discussion

The Flores earthquake represents the first seismological evidence that active thrusting occurs behind the Sunda Arc north of Flores. We suggest that the south dipping nodal plane is the fault plane because the strike of this plane agrees better with the local strike of the Flores Thrust than does the strike of the steeper plane and the sense of relative displacement (southside

up) on the Flores Thrust is documented in seismic reflection profiles (Figure 5a and Silver et al. [1983]). Furthermore, as shown above, gravity evidence suggests that the Flores Basin crust dips toward and continues under the deformed sediments tens of kilometers south of the thrust zone.

The south dipping nodal plane for the 1978 earthquake dips to the SSW at about  $30^\circ$ . This angle is significantly steeper than the  $6^\circ$  dip of the Flores Basin crust beneath the accreted wedge determined from gravity data and from the dip of planar sediments observed in the reflection profile of Figure 5a. Similarly, along the Philippine Trench, Cardwell et al. [1980] found the dip of the seismic zone defined by earthquake hypocenters and fault planes from shallow thrust events to be  $24 \pm 10^\circ$  in the north to  $45 \pm 15^\circ$  in the south, although the events examined occurred only 50-100 km landward of the trench. The Philippine Trench is associated with a seismic zone extending to only 150-km depth and is not associated with active volcanism; it is therefore thought to be quite young [Cardwell et al., 1980]. The projections of the Philippine and the New Hebrides seismic zones are shown in Figure 6a for comparison and indicate that the slip angle and position of the Flores earthquake (shown by a star) with respect to the trench are consistent with the subduction interpretation within the limits imposed by observations in other parts of the world.

Silver et al. [1983] discuss the relative

importance of possible driving mechanisms and present arguments in favor of continent collision as the primary driving force in the development of back arc thrusting behind the eastern Sunda Arc. The azimuth of the slip vector (which is well constrained) for the 1978 earthquake provides strong support for this interpretation. Although the strike of the fault plane for the 1978 earthquake parallels the NW trending bathymetric expression of the Flores Thrust, the slip vector is oriented nearly north-south (Figure 2), or in the same direction as the relative plate motion between the Indian Ocean-Australia plate and the eastern Sunda Arc (azimuth  $0^\circ$ ) [Cardwell et al., 1981].

The distinction between the possible mechanisms of back arc thrusting (shallow dipping decollement as opposed to high-angle imbricate thrusting) has important bearing on the evolution of the convergent margin. It is clear from the tectonic development of western Canada, the western United States, and the Andes that both styles of deformation in the back arc region can occur in an "Andean" setting. The implications of either case are even greater, however, when thrusting involves oceanic lithosphere because its negative buoyancy will lead to subduction if a length sufficient to overcome resisting forces is pushed into the asthenosphere [McKenzie, 1977]. Of the two models presented here for the back arc thrust north of Flores, the case of decollement may lead to subduction, whereas high-angle imbricate thrusting would result in crustal thickening possibly followed by uplift and ophiolite emplacement.

We favor the decollement (subduction) model for the back arc thrust zone. The strongest evidence is the presence of only a single major thrust fault along the length of the thrust zone [Silver et al., 1983]. South of the Flores Thrust there is a noticeable lack of undeformed sediments astride the deformed wedge (Figure 5a) despite the abundance of active volcanic activity to the south. This observation implies that deformation continues within the wedge, but there are no indications of major south dipping faults cutting the deformed wedge, as is predicted by the imbricate thrust model. Thus the deformation within the wedge is probably in response to shear at its base [Davis et al., 1983], along a plane that crops out at the Flores Thrust. The smoothness of the gravity field over the deformed wedge also indicates that there are no major crustal offsets south of the frontal thrust.

A second argument is based on the mechanics of thrusting: what is the source of the stress maintaining the gravity lows? The low gravity values cannot be due to thickened crust that remains in isostatic equilibrium and therefore indicates deflection of the underthrusting plate. The load causing deflection will be supported by the plate's flexural strength and therefore associated with a gravity high [Lyon-Caen and Molnar, 1983; Karner and Watts, 1983]. The free-air gravity anomalies over the Flores Basin south of the Flores Thrust become positive at about km 130 (Figure 5a), suggesting that the load deflecting the Flores Basin lithosphere is south of this point. Thus the underthrusting plate (or thrust sheets) must exist beneath Flores Island. The fact that no imbricate thrust

sheets are observed on Flores (faulting beneath Flores Island is predominantly strike slip) is therefore a strong argument against the imbricate thrust model.

Although it is not possible at present to say with much confidence whether or not the observed thrusting is, or will eventually become, a self-sustaining subduction system in the sense that the negative buoyancy of the lithospheric mantle being shoved into the asthenosphere overtakes forces resisting subduction (i.e., buoyancy of the crust, friction on the thrust surface, and resistance to bending), we suggest that the conditions behind the eastern Sunda Arc are favorable for this to occur. Because the arc is still volcanically active, the lithosphere is probably fairly warm and weak, offering diminished frictional resistance to thrusting. In addition, volcanic activity causes high sedimentation rates behind the arc, and plate deflection will be infilled by sediments (see Figure 5a) rather than water placing an additional load on the depressed plate. Finally, the northward motion of the Australian continent relative to the Indonesian Islands provides a rapid and long-term driving mechanism for the back arc thrusting. Although little oceanic crust exists north of Flores to feed the newly developing subduction system, further east the Banda Sea contains several hundred kilometers of oceanic crust that could eventually be subducted southward beneath the Banda Arc and therefore constitute a true arc polarity reversal.

Acknowledgments. We thank Eli Silver and M. Untung for allowing us to use their gravity data. We also thank Anne Tréhu, Eli Silver, Peter Molnar, and two AGU reviewers for valuable comments and criticisms, and Sarah Luria for help with preparation of the manuscript. This work was supported by NSF grant EAR-8115909 and by the Advanced Research Projects Agency of the Department of Defense, monitored by the Air Force Office of Scientific Research under grant F 49620-82-K-0004.

#### References

- Bowin, C.O., G.M. Purdy, C. Johnston, G.G. Shor, L. Lawver, H.M.S. Hartono, and P. Jezek, Arc-continent collision in the Banda Sea region, Am. Assoc. Petrol. Geol. Bull., **64**, 868-915, 1980.
- Cardwell, R.K., and B.L. Isacks, Geometry of subducted lithosphere beneath the Banda Sea in eastern Indonesia from seismicity and fault plane solutions, J. Geophys. Res., **83**, 2825-2838, 1978.
- Cardwell, R.K., B.L. Isacks, and D.E. Karig, The spatial distribution of earthquakes, focal mechanism solutions and plate boundaries in the Philippine and northeastern Indonesian islands, in The Tectonic and Geologic Evolution of Southeast Asian Sea and Islands, Geophys. Monogr. Ser., vol. 23, pp. 1-36, edited by D.E. Hayes, AGU, Washington, D. C., 1980.
- Cardwell, R.K., E.S. Kappel, M.S. Lawrence and B.L. Isacks, Plate convergence along the Indonesian arc (abstract), Eos Trans. AGU, **62**, 404, 1981.

- Christensen, N.I., and M.H. Salisbury, Structure and constitution of the lower oceanic crust, Rev. Geophys. Space Phys., **13**, 57-86, 1975.
- Curry, J.R., G.G. Shor, R.W. Raitt, and M. Henry, Seismic refraction and reflection studies of crustal structure of the eastern Sunda and western Banda arcs, J. Geophys. Res., **82**, 2479-2489, 1977.
- Davis, D., J. Suppe, and F.A. Dahlen, Mechanics of fold-and-thrust belts and accretionary wedges, J. Geophys. Res., **88**, 1153-1172, 1983.
- Dewey, J.F., and J.M. Bird, Mountain belts and the new global tectonics, J. Geophys. Res., **75**, 2625-2647, 1970.
- Dewey, J.W., Seismicity studies with the method of joint hypocenter determination, Ph.D. thesis, 124 pp., Univ. of Calif., Berkeley, 1971.
- Geological Research and Development Centre, 1983 Annual Report, Bandung, Indonesia, in preparation, 1984.
- Grow, J.A., and C.O. Bowin, Evidence for high density crust and mantle beneath the Chile Trench due to descending lithosphere, J. Geophys. Res., **80**, 1449-1458, 1975.
- Hamilton, W., Tectonics of the Indonesian region, U. S. Geol. Surv. Prof. Pap. **1078**, 345 pp., 1979.
- Hodgson, J.H., A short-period seismograph network in southeast Asia, Bull. Seismol. Soc. Am., **70**, 385-392, 1980.
- Jacobson, R.S., G.G. Shor, R.M. Kieckhefer and G.M. Purdy, Seismic refraction and reflection studies in the Timor-Aru trough system and Australian continental shelf, Mem. Am. Assoc. Petrol. Geol., **29**, 209-222, 1979.
- Johnson, R.W., and A.L. Jaques, Continent-arc collision and reversal of arc polarity: New interpretation from a critical area, Tectonophysics, **63**, 111-124, 1980.
- Johnson, T., and P. Molnar, Focal mechanisms and plate tectonics of the southwest Pacific, J. Geophys. Res., **77**, 5000-5032, 1972.
- Karner, G.D., and A.B. Watts, Gravity anomalies and flexure of the lithosphere at mountain ranges J. Geophys. Res., **88**, 10449-10477, 1983.
- Langston, C.A., Source inversion of seismic waveforms: The Koyna, India, earthquakes of 13 September 1967, Bull. Seismol. Soc. Am., **71**, 1-24, 1981.
- Lyon-Caen, H., and P. Molnar, Constraints on the structure of the Himalaya from an analysis of gravity anomalies and a flexural model of the lithosphere, J. Geophys. Res., **88**, 8171-8191, 1983.
- McCaffrey, R., and R. Sutardjo, Reconnaissance microearthquake survey of Sulawesi, Indonesia, Geophys. Res. Lett., **9**, 793-796, 1982.
- McKenzie, D.P., Speculations on the consequences and causes of plate motion, Geophys. J. R. Astron. Soc., **18**, 1-18, 1969.
- McKenzie, D.P., The initiation of trenches: A finite amplitude instability, in Island Arcs, Deep Sea Trenches and Back-Arc Basins, Maurice Ewing Ser., vol. 1, edited by M. Talwani and W.C. Pitman III, pp. 57-61, AGU, Washington, D. C., 1977.
- Moore, G.F., and E.A. Silver, Collision processes in the northern Molucca Sea, in The Tectonic and Geologic Evolution of Southeast Asian Seas and Islands, Part 2, Geophys. Monogr. Ser., vol. 23, edited by D.E. Hayes, pp. 360-372, AGU, Washington, D. C., 1983.
- Nábělek, J.L., Determination of earthquake source parameters from inversion of body waves, Ph.D. thesis, Mass. Inst. of Technol., Cambridge, 1984.
- Nafe, J.E. and C.L. Drake, Physical properties of marine sediments, in The Sea, vol. 3, edited by M.N. Hill, pp. 794-815, John Wiley, New York, 1963.
- Silver, E.A., and J.C. Moore, The Molucca Sea collision zone, Indonesia, J. Geophys. Res., **83**, 1681-1691, 1978.
- Silver, E.A., D.R. Reed, R. McCaffrey, and Y. Joyodiwiryo, Backarc thrusting in the eastern Sunda Arc, Indonesia: A consequence of arc-continent collision, J. Geophys. Res., **88**, 7429-7448, 1983.
- Stewart, G.S., and S.N. Cohn, The 1976 August 16, Mindanao, Philippine earthquake ( $M_s=7.8$ )-- Evidence for a subduction zone south of Mindanao, Geophys. J. R. Astron. Soc., **57**, 51-65, 1979.
- Tréhu, A.M., J.L. Nábělek, and S.C. Solomon, Source characterization of two Reykjanes Ridge earthquakes: Surface waves and moment tensors; P waveforms and nonorthogonal nodal planes, J. Geophys. Res., **86**, 1701-1724, 1981.
- Usna, I., S. Tjokrosapoetro, and S. Wiryosujono, Geological interpretation of a seismic reflection profile across the Banda Sea between Wetar and Buru Islands, Bull. Geol. Res. Dev. Centre, **1**, 7-15, 1979.
- von der Borch, C.C., Continent-island arc collision in the Banda arc, Tectonophysics, **54**, 169-193, 1979.
- Ward, S.N., A technique for the recovery of the seismic moment tensor applied to the Oaxaca, Mexico, earthquake of November 1978, Bull. Seismol. Soc. Am., **70**, 717-734, 1980.
- Watts, A.B., and M. Talwani, Gravity anomalies seaward of deep-sea trenches and their tectonic implications, Geophys. J. R. Astron. Soc., **36**, 57-90, 1974.

R. McCaffrey and J. Nábělek, Department of Earth, Atmospheric, and Planetary Sciences, Massachusetts Institute of Technology, Cambridge, MA 02139

(Received August 12, 1983;  
revised March 5, 1984;  
accepted March 23, 1984.)